

Dynamic Hyperparameter Importance for Efficient Multi-Objective Optimization

Daphne Theodorakopoulos^{1,2}, Marcel Wever^{1,2} and Marius Lindauer^{1,2}

¹Institute of Artificial Intelligence (LUH|AI), Leibniz University Hannover

²L3S Research Center

{d.theodorakopoulos, m.wever, m.lindauer}@uni-hannover.de

Abstract

Choosing a suitable ML model is a complex task that can depend on several objectives, e.g., accuracy, model size, fairness, inference time, or energy consumption. In practice, this requires trading off multiple, often competing, objectives through multi-objective optimization (MOO). However, existing MOO methods typically treat all hyperparameters as equally important, overlooking that hyperparameter importance (HPI) can vary significantly depending on the trade-off between objectives. We propose a novel dynamic optimization approach that prioritizes the most influential hyperparameters based on varying objective trade-offs during the search process, which accelerates empirical convergence and leads to better solutions. Building on prior work on HPI for MOO post-analysis, we now integrate HPI, calculated with HyperSHAP, into the optimization. For this, we leverage the objective weightings naturally produced by the MOO algorithm ParEGO and adapt the configuration space by fixing the unimportant hyperparameters, allowing the search to focus on the important ones. Eventually, we validate our method with diverse tasks from PyMOO and YAHPO-Gym. Empirical results demonstrate improvements in convergence speed and Pareto front quality compared to baselines.

1 Introduction

Hyperparameter optimization (HPO) is a critical step in maximizing the performance of machine learning models [Bergstra and Bengio, 2012; Snoek *et al.*, 2012; Lévesque *et al.*, 2016; Feurer and Hutter, 2019; Bischl *et al.*, 2023]. Traditionally, HPO has been conducted with a single performance objective in mind, often predictive accuracy. However, real-world applications rarely depend solely on accuracy. Instead, they must balance multiple, often conflicting requirements. For example, large-scale deployments demand low inference latency, embedded and edge devices require strict limits on memory and energy usage; in socially sensitive applications, fairness constraints may be mandated by regulation [Schmucker *et al.*, 2020; Weerts *et al.*, 2024]. This moti-

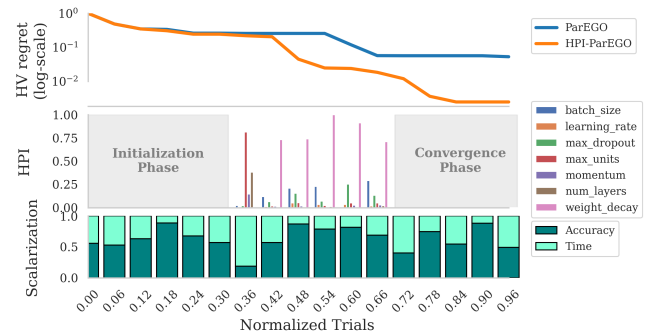


Figure 1: The plot shows the HPO task `lcbench_12605` for one seed, trading off accuracy vs time, the top plot compares ParEGO with our improved variant with dynamic HPI consideration, the middle shows changing HPI for the different scalarizations, which are shown in the bottom. There is an initialization and a convergence phase, during which no configuration space reduction is performed.

vates the need to frame HPO as a multi-objective optimization (MOO) problem, where the goal is not a single best configuration but an approximation of the Pareto front, a set of optimal trade-offs across objectives. From that, a developer can make an informed decision about the final model to deploy.

Compared to single-objective HPO, multi-objective variants are considerably more complex and computationally demanding, making efficiency critical. While existing MOO methods [Elsken *et al.*, 2019; Yiyang *et al.*, 2021; Morales-Hernández *et al.*, 2022] assume uniform HPI, single-objective studies show that HPI varies by task [Bergstra and Bengio, 2012; Hutter *et al.*, 2014; van Rijn and Hutter, 2018; Wever *et al.*, 2026]. Leveraging this variability in HPI can improve optimization efficiency [Wang *et al.*, 2025].

Recent work shows that HPI varies across different objective trade-offs in multi-objective settings [Theodorakopoulos *et al.*, 2024]. We hypothesize that optimizers with dynamic scalarization, such as ParEGO [Knowles, 2006], can exploit this by adapting their search toward the most relevant hyperparameters. Our approach realizes this by dynamically subsampling the configuration space according to the current scalarization. Figure 1 displays the superior performance of our optimizer against the baseline in an illustrative example.

Contributions

1. We present the first integrated method for efficient multi-objective optimization (MOO) that dynamically incorporates HPI into the optimization loop of scalarization-based MOO approaches. The method adaptively selects and focuses on the most influential hyperparameters based on the current objective scalarization.
2. We provide insights into the performance of our method with a diverse set of synthetic and HPO tasks from PyMOO [Blank and Deb, 2020] and YAHPO-Gym [Pflisterer *et al.*, 2022]. Our HPI-based hyperparameter subsampling outperforms standard ParEGO and other popular MOO baselines in terms of convergence speed and Pareto front quality.
3. We demonstrate the impact of key design choices through an ablation study, which includes the amount of randomness, HPI subsampling thresholds, when to draw a new scalarization, and configuration space adaptation.

2 Background and Related Work

This section reviews basic concepts and prior work relevant to our approach, covering three main areas: (i) multi-objective hyperparameter optimization, (ii) hyperparameter importance, and (iii) dynamic configuration space adaptation.

2.1 Multi-Objective HPO

Multi-objective optimization (MOO) optimizes two or more potentially conflicting objectives simultaneously. Unlike single-objective optimization, MOO does not produce a single solution, but a *set* of Pareto-optimal solutions, where no objective can be improved without degrading another [Pareto, 1971]. This set, known as the Pareto front, represents the trade-off surface among objectives:

$$\begin{aligned} \min_{\mathbf{x} \in \mathcal{X}} \mathbf{f}(\mathbf{x}) &= (f_1(\mathbf{x}), \dots, f_m(\mathbf{x})) \\ \text{subject to: } &\neg \exists \mathbf{x}' \in \mathcal{X} \text{ such that } f_i(\mathbf{x}') \leq f_i(\mathbf{x}) \forall i, \\ &\text{with } f_j(\mathbf{x}') < f_j(\mathbf{x}) \text{ for some } j \end{aligned} \quad (1)$$

In hyperparameter optimization (HPO), MOO is often tackled using either evolutionary algorithms or Bayesian optimization [Morales-Hernández *et al.*, 2022]. A well-known and frequently used evolutionary approach is NSGA-II [Deb *et al.*, 2002], which maintains solution diversity and convergence through non-dominated sorting and crowding distance.

Among Bayesian optimization methods, ParEGO [Knowles, 2006] is widely used. It converts a multi-objective problem into a single-objective one by randomly sampling scalarization weights, enabling standard surrogate-based optimization techniques:

$$\min_{\lambda \in \Lambda} \left\{ \max_{j=1, \dots, m} [w_j \cdot f_j(\lambda)] + \rho \sum_{j=1}^m w_j \cdot f_j(\lambda) \right\} \quad (2)$$

where $\lambda \in \Lambda$ represents a candidate configuration from the configuration space Λ , $f_j(\lambda)$ denotes the j -th objective function to be minimized, $\mathbf{w} = (w_1, \dots, w_m)$ is a weight vector

sampled randomly, where $w_j \geq 0$ and $\sum_{j=1}^m w_j = 1$, and ρ is a small positive scalar (e.g., 0.05) that encourages diversity in the optimization process.

While efficient, ParEGO and similar MOO algorithms typically treat all hyperparameters equally, ignoring the fact that some may have more impact than others depending on the objective trade-off. Our work embeds dynamic HPI estimation into the ParEGO framework to prioritize the most relevant hyperparameters during optimization, improving both convergence speed and solution quality.

2.2 Hyperparameter Importance (HPI)

In single-objective HPO, a variety of HPI methods have been developed to estimate the importance of individual hyperparameters. These are typically applied post-hoc, using the results of completed optimization runs. To this end, surrogate models trained on such optimization data are often employed to model performance as a function of hyperparameter configurations. Notable techniques include fANOVA [Hutter *et al.*, 2014], forward selection [Hutter *et al.*, 2013], and Local Parameter Importance [Biedenkapp *et al.*, 2018], which assess importance by decomposing performance variance. Shapley values [Shapley, 1953] have also been applied to attribute importance in Bayesian optimization [Adachi *et al.*, 2023; Rodemann *et al.*, 2024; Wever *et al.*, 2026]. As a more local approach, ablation path analysis [Fawcett and Hoos, 2016; Biedenkapp *et al.*, 2017] measures hyperparameter contributions by comparing the default configuration to optimized ones. Studies, e.g., by van Rijn and Hutter [2018], Probst *et al.* [2019], and Moussa *et al.* [2024] have explored HPI across datasets, providing insights into general patterns of hyperparameter relevance.

Building on these foundations, Theodorakopoulos *et al.* [2024] extended HPI estimation to the multi-objective setting via a post-hoc analysis framework. Their approach scalarized objective values from the Pareto front and applied fANOVA and ablation analysis to evaluate importance retrospectively. While insightful for different objective trade-offs, this method does not influence the optimization process itself. Our work advances this line of research by integrating HPI estimation directly into the optimization, enabling dynamic and adaptive search guidance.

2.3 Dynamic Configuration Space Adjustments

Several HPO methods dynamically adjust the configuration space to improve efficiency. For instance, Wistuba *et al.* [2015] prune unpromising regions using prior experiments on other datasets or early evaluations, while Lee *et al.* [2022] adapt the space under time constraints by shrinking or expanding it as the budget evolves. Tools like Optuna [Akiba *et al.*, 2019] allow users to manually intervene during optimization. More closely related to our approach, ExperienceThinking [Wang *et al.*, 2021] applies HPI estimation in a single-objective setting to ignore unimportant hyperparameters and dynamically reduce the configuration space. Basu *et al.* [2025] include human priors per objective in the acquisition function of MOO to speed up the optimization. While they rely on user-defined beliefs to adjust the search, our approach automatically adapts the search using HPI on the fly.

Moreover, we do not adjust the acquisition function; only the configuration space is modified. Their per-objective priors cover only the extremes of the Pareto front, while our scalarization-based HPI-ParEGO explores a broader region.

These efforts reflect a growing interest in adaptive HPO techniques that tailor the configuration space to improve search efficiency and efficacy. However, to the best of our knowledge, no prior work incorporates dynamic HPI estimation into multi-objective HPO. Our method closes this gap by estimating HPI dynamically, based on scalarized objectives, and guiding the search toward more promising regions of the configuration space in a data-driven way.

3 Dynamic Hyperparameter Subsampling

We extend the ParEGO algorithm for multi-objective HPO by incorporating HPI estimation into each optimization step. Our method dynamically identifies the most influential hyperparameters under the current objective scalarization and uses this information to guide the search. Section 3.1 outlines the overall approach, Section 3.2 details HPI integration; Section 3.3 describes configuration space adaptation, and Section 3.4 presents the thresholding strategy. An overview of the algorithm is shown in Figure 2.

3.1 General Algorithm: HPI-ParEGO

Our method builds on ParEGO [Knowles, 2006], a Bayesian optimization approach to multi-objective problems.¹ Instead of optimizing all objectives simultaneously, ParEGO repeatedly scalarizes them with a weighted Tchebycheff function, see Section 2.1, turning the task into a sequence of single-objective subproblems. By focusing on different trade-offs at each iteration, it gradually explores a diverse set of solutions along the Pareto front.

The process begins with an initial design of sampled configurations (Line 1 in Algorithm 1). Every u iterations, ParEGO samples a new set of weights w uniformly at random from the unit simplex (Lines 3-4), which determines the emphasis placed on each objective. Based on the current optimization history \mathcal{H} , which includes previously evaluated configurations λ_i and their performance values $f(\lambda_i)$, ParEGO fits a surrogate model $\hat{f}: \lambda \mapsto f(\lambda_i)$ (Line 5). This model approximates how different configurations are expected to perform under the chosen scalarization.

Following a similar line of thought to interleaving randomly sampled configurations in Bayesian Optimization, with a random chance r , we evaluate a random configuration from the original full configuration space (Line 6-7). We do this not only to exploit the information on HPI gained from a restricted configuration space, which risks premature convergence or overfitting to early importance estimates, but also to generate new information on the optimization problem. This could also help the surrogate model improve on hyperparameters that are underexplored since they were not part of the

¹In principle, our approach only assumes that the objectives are dynamically scalarized during the optimization, and thus is applicable to approaches similar to ParEGO [Zhang and Li, 2007; Bradford *et al.*, 2018] with at most minor modifications. For the sake of clarity and simplicity, we focus on ParEGO in our paper.

Algorithm 1: HPI-ParEGO

Input: Objective functions $f(\cdot) = (f_1(\cdot), \dots, f_m(\cdot))$, configuration space Λ , acquisition function α , budget B , initial size N_{init} , threshold τ , random chance r , weight update every u iterations

Output: Approximated Pareto Set

```

1 Initialize history  $\mathcal{H} = \{(\lambda_i, f(\lambda_i))\}_{i=1}^{N_{\text{init}}}$  with an initial
  design (e.g., random search)
2 for  $i = N_{\text{init}} + 1$  to  $B$  do
3   if  $i \bmod u = 0$  then
4     | Update scalarization weights  $w \sim \Delta^{m-1}$ 
5     Train surrogate model  $\hat{f}_w$  on  $\mathcal{H}$  using the scalarized
6     objective value of ParEGO (see Equation 2)
7     if  $r\%$  chance then
8       | Evaluate random configuration  $f(\lambda)$  from original
9       | configuration space  $\lambda \in \Lambda$ 
10    else
11      | Compute HPI  $h(\Lambda^j)$  for each hyperparameter  $\Lambda^j$ 
12      | // See Section 3.2
13      | Select important hyperparameters (HPs) by HPI
14      | threshold  $\tau$  based on  $h(\Lambda^j)$ 
15      | Adapt configuration space  $\Lambda' \subset \Lambda$  by fixing
16      | unimportant HPs // see Section 3.3
17      | Select configurations:
18      |  $\lambda_i \in \arg \max_{\lambda \in \Lambda'} \alpha(\lambda | \mathcal{H}, \hat{f}_w)$ 
19      | Evaluate  $f(\lambda_i)$ 
20      Add result to history:  $\mathcal{H} \leftarrow \mathcal{H} \cup \{(\lambda_i, f(\lambda_i))\}$ 
21      Update threshold  $\tau$  // See Section 3.4
22 return Pareto Set based on  $\mathcal{H}$ 

```

important hyperparameters so far, but might be relevant for another scalarization.

We extend this loop by incorporating HPI (Lines 9-11). Using the surrogate model \hat{f} , we estimate how important each hyperparameter is for the current scalarized objective, assigning an importance score $h(\Lambda^j)$ to each hyperparameter Λ^j . We then select only the relevant hyperparameters by applying a threshold τ (Line 10) and reduce the configuration space accordingly to $\Lambda' \subset \Lambda$ (Line 11). Less important hyperparameters are fixed to a constant value (i.e., the current incumbent configuration in our implementation), allowing the algorithm to focus on the influential dimensions.

Next, the acquisition function α , trading off exploration and exploitation, e.g., expected improvement [Jones *et al.*, 1998] or upper confidence bound [Srinivas *et al.*, 2010], is optimized over the reduced space Λ' to propose new candidate configurations (Lines 12). The top configurations are then evaluated on the actual objectives, and the result is added to the history \mathcal{H} (Lines 13-14). Finally, the threshold τ for selecting important hyperparameters may be updated based on the progress of the optimization (Line 15).

3.2 Calculating MO-HPI

To streamline optimization, we dynamically estimate HPI, focusing on the dimensions most likely to improve performance. Since hyperparameter relevance varies with the objective weighting [Theodorakopoulos *et al.*, 2024], the set of important hyperparameters is re-evaluated whenever the

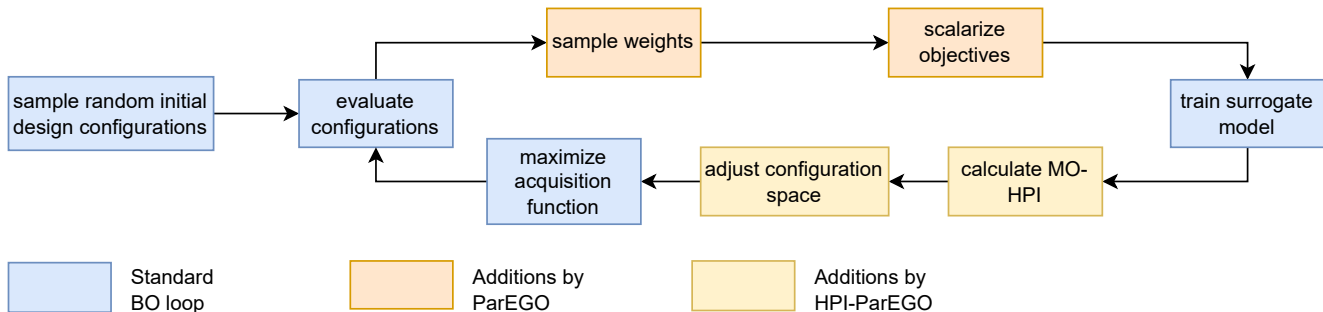


Figure 2: Algorithm overview: Blue corresponds to the normal Bayesian optimization (BO) loop, orange to the ParEGO algorithm, and yellow to the HPI-ParEGO additions proposed in this work.

weights change, making the choice of HPI method critical.

We use HyperSHAP [Wever *et al.*, 2026], a recent HPI method quantifying tunability [Probst *et al.*, 2019] based on Shapley values and interactions. Unlike HPI methods such as fANOVA, which quantify how much a hyperparameter explains the variance in performance (incl. performance degradation), HyperSHAP quantifies how much changing its value from a default (in our case, incumbent value) improves performance. This makes HyperSHAP especially relevant in optimization settings where we want to identify which hyperparameters to prioritize. It can summarize higher-order interactions in a principled way, facilitating decision-making in our method without ignoring such dependencies.

Technically, HyperSHAP models the HPO process as a cooperative game [Fudenberg and Tirole, 1991], where each hyperparameter acts as a “player” contributing to the outcome. Shapley values are used to estimate the marginal contribution of each hyperparameter to the performance predicted by a surrogate model \hat{f} trained on the current run history. Within the multi-objective setting, we leverage the trait of ParEGO to scalarize the objectives into single-objective problems.

Since the Shapley values represent the marginal contribution, they can be summed to represent the maximum improvement over the reference configuration. We reduce the configuration space by selecting those hyperparameters that are jointly responsible for $\tau\%$ of the performance gain. We order the hyperparameters by maximal contribution and select the top hyperparameters until the sum of important hyperparameters surpasses the threshold of τ times the maximal improvement (sum of all Shapley values). If another non-additive HPI method is used, alternatively, the τ -quantile of all HPI scores can be used to select the most important hyperparameters.

3.3 Adjusting the Configuration Space

We consider only the most influential hyperparameters and reduce optimization complexity by constructing a reduced configuration space $\Lambda' \subset \Lambda$, by diminishing the influence of less important hyperparameters. Based on the importance scores $h(\Lambda^j)$, we retain only the most relevant hyperparameters $\Lambda' \subset \Lambda$ and fix the rest to constants (we use the incumbent). Each reduction starts from the original configspace Λ . In rare cases, this reduction leads to a too narrow configuration space, such that no new configurations can be generated; we then fall back to the original space Λ for that iteration.

3.4 Dynamic Threshold

The threshold τ determining the important hyperparameters is not fixed but changes over the course of the optimization. In principle, one could bring up two lines of arguments:

- (i) The optimizer should start with a very restricted space to make quick progress in the beginning and later on, the space should be less constrained to allow for optimal fine-tuning;
- (ii) or the optimizer should be first allowed to consider all hyperparameters to directly learn which hyperparameters are important and to let the surrogate model improve, and later on, the space is constrained based on sufficient information.

In fact, we argue that both lines of arguments are reasonable and thus, we propose a combination to get the best of both worlds: First, we disable subsampling during the initial third of trials, allowing broad exploration and learning of HPI (initialization phase), then we apply a threshold of $\tau = 0.8$, corresponding to 80% of the sum of Shapley values for the next third of trials to focus the search on the most relevant hyperparameters and make quick progress. Finally, in the last third of trials, we reconsider all hyperparameters, allowing tuning even on the less important ones (convergence phase). We call this approach “Symmetric-0.8”.

4 Empirical Evaluation

In the following, we describe our experimental setup and then evaluate our method following these research questions:

1. Is our hyperparameter-importance-based approach more effective than the standard ParEGO algorithm (and other MO-optimizers) on well-understood artificial benchmark functions? (Section 4.2)
2. How do the design choices of HPI-ParEGO impact its performance? (Section 4.3)
3. How well do the results translate to real-world HPO benchmarks? (Section 4.4)

4.1 Experiment Setup

Datasets. Our experiments are conducted using artificial functions from PyMOO [Blank and Deb, 2020] and HPO tasks from YAHPO-Gym [Pfisterer *et al.*, 2022]. These benchmarks have varying dimensionalities in their configuration spaces. From PyMOO, we selected the ZDT tasks [Zitzler *et al.*, 2000], except for ZDT5, as it is defined in a discrete bitstring domain rather than a continuous domain, which

makes the conversion to an HPO problem more challenging. We selected 13 tasks from `LCBench` [Zimmer *et al.*, 2021] and 13 tasks from `rbv2_ranger`, both from the YAHPO-Gym, based on the property that different hyperparameters are important for different objective tradeoffs, for details, see Appendix A. Of these, three tasks from each scenario were used for an initial ablation study, and the remaining 20 were used for an unbiased final evaluation.

Baselines. The ParEGO implementation in the HPO framework SMAC3 [Lindauer *et al.*, 2022] without our HPI modifications serves as our primary baseline. A random forest is used as a surrogate model and the acquisition function is expected improvement which showed strong baseline performance in prior HPO benchmark studies [Eggenberger *et al.*, 2021]. The surrogate model is retrained after two new configurations have been evaluated (instead of every configuration due to computational constraints), and the weights are updated every ten iterations ($u = 10$). Moreover, the random chance r to evaluate a random configuration is set to 10%. Finally, the first configuration is always the default configuration. Our HPI-ParEGO variant uses the same settings to eliminate confounding factors. In addition, we include common MOO algorithms in the comparison: Multi-objective TPE [Ozaki *et al.*, 2020] and NSGA-II [Deb *et al.*, 2002], both implemented in Optuna [Akiba *et al.*, 2019], as well as DE from Nevergrad [Rapin and Teytaud, 2018].

Evaluation Metrics. To compare the optimizers across tasks and seeds, we compute the normalized incumbent cost of the best-so-far configuration over time. For that, we negate the hypervolume (HV), which is the area behind the current Pareto front, and apply min-max normalization per task, resulting in a standardized $[0, 1]$ scale where lower values indicate better performance. We compute a reference point by taking the maximum of all observed cost vectors per task, representing the worst-case as a bounding point for HV calculation. We generate convergence plots, which plot the normalized incumbent HV regret over the number of normalized trials (i.e., function evaluations, or model trainings and evaluations), first averaged by tasks and then by seeds to obtain uncertainties across random seeds. As a metric for any time performance, we use the mean area under the curve (AUC) of the convergence plot of each task and seed.

Implementation Details. Appendix B details our hardware usage. We repeated our experiments with 10 random seeds; in the ablation study, we used 5 seeds. Appendix C details for how many trials each task was executed. More implementation details can be found in Appendix D. We use the CARP-S benchmark suite library [Benjamins *et al.*, 2025] to execute our experiments.

4.2 HPI-ParEGO on PyMOO

First, we evaluate our approach on the selected PyMOO tasks (Figure 3). The PyMOO tasks are established artificial MOO functions, allowing us to study the optimizers in detail. The results show that the HPI-ParEGO optimizer begins to outperform the ParEGO baseline already at a bit more than 30% of the tasks’ number of trials, which is where the HPI-based reduction begins. This indicates that, according to

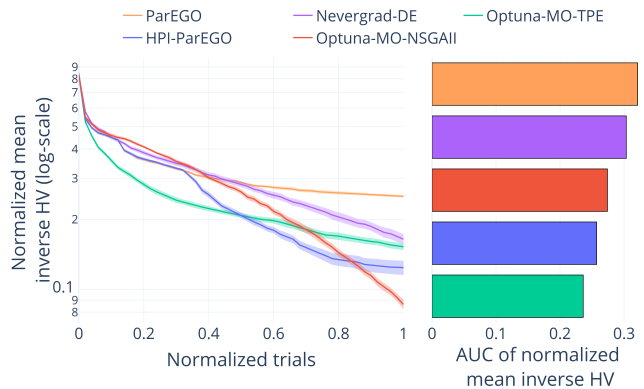


Figure 3: Results of the HPI-ParEGO optimizer compared to all baselines on the PyMOO tasks.

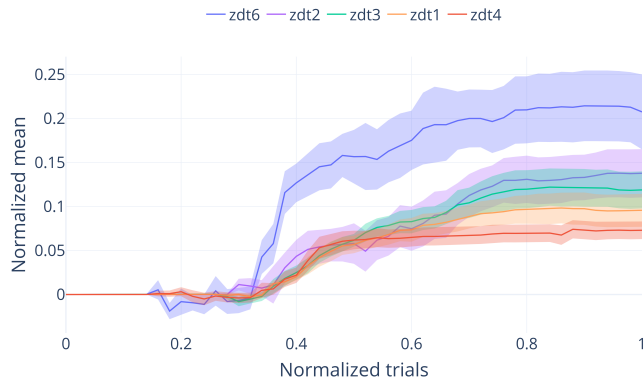


Figure 4: Comparing the HPI-ParEGO optimizer to the ParEGO baseline on PyMOO per task. Values > 0 indicate a better performance of HPI-ParEGO.

the “Symmetric-0.8” strategy (see Subsection 3.4), it quickly identified the most important hyperparameters to reduce the configuration space. Initially, and as shown in the AUC plot, the MO-TPE optimizer outperforms the HPI-ParEGO optimizer; however, after approximately half of the trials, HPI-ParEGO performs best, only being outperformed by NSGA-II in the final stages.

To provide further insights into the behavior of each of the functions, Figure 4 details the per-task performance differences between HPI-ParEGO and ParEGO. Across all PyMOO tasks, HPI-ParEGO substantially surpasses the baseline on every function. These findings underline the potential of HPI-ParEGO in handling well-known benchmark problems and its ability to accelerate convergence.

4.3 Ablation Study

Second, we designed an ablation study to address our next research question: how do the design choices of HPI-ParEGO impact its performance? To this end, we systematically varied each component of the algorithm as outlined in Table 1, modifying one aspect at a time while keeping the others fixed to the default configuration of our proposed method. We show the results on three tasks from `LCBench` and three from

Table 1: Explored Settings for the HPI-ParEGO Algorithm. 0 corresponds to no reduction in that third of trials.

Component	Values
Adjust configspace	incumbent, default, random
Threshold τ	Initialization phase (0,0.8,0.8), Convergence phase (0.8,0.8,0), Constant-0.8, Symmetric-0.8
Random chance r	0.0, 0.1, 0.2
Weight update iterations u	6, 10, 20

rbv2_ranger, which are excluded from evaluation to avoid overfitting our optimizer. This allows us to isolate and quantify the contribution of each component to its efficiency.

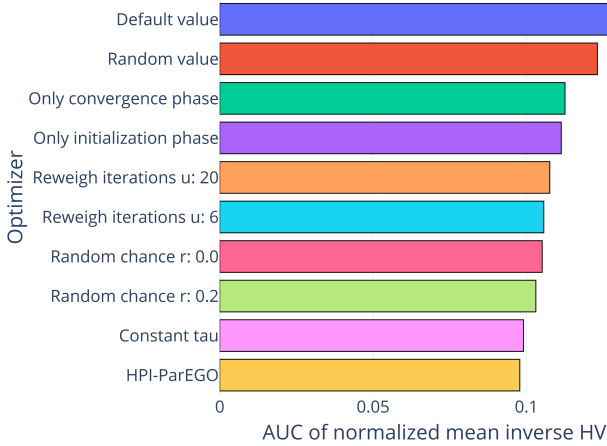


Figure 5: Ablation results overview of all settings.

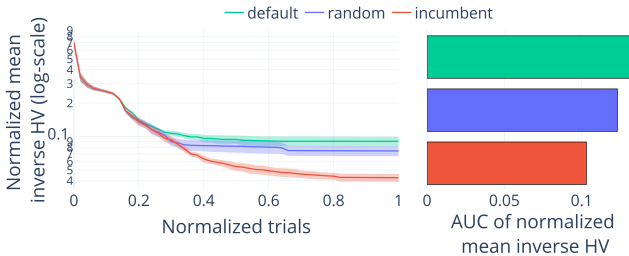


Figure 6: Ablation results for different constant values to adjust the configuration space.

The results of the entire ablation study are summarized in Figure 5. The plot shows the AUC when altering one component from the default HPI-ParEGO. The biggest improvement can be seen by setting the unimportant hyperparameters to their current incumbent value (see also Figure 6). We tested setting the constant values of the unimportant hyperparameters to the hyperparameter’s default value, the configuration with the current incumbent value in the run history \mathcal{H} for the given scalarization, or a randomly sampled value. Additionally, for HyperSHAP, that choice (incumbent, default, or random) was also used as a reference configuration.

Full results for the other components are provided in Appendix D. The choice of threshold τ has a positive influence;

however, the constant threshold performs similarly at later stages of the optimization. Nevertheless, it is definitely worse until around 60% of the trials. This means that using the full space at the beginning is more important than using it at the end. Using random importance values sometimes and the weight update iterations has a smaller but positive influence on the performance.

4.4 HPI-ParEGO on HPO Benchmarks

Lastly, we go to HPO problems and compare the HPI-ParEGO optimizer against the ParEGO baseline and additional baseline optimizers on the selected tasks of YAHPO-Gym. The results, summarized in Figure 7 for the LCBench tasks and in Figure 8 for rbv2_ranger, highlight the advantages of our HPI-guided approach. In contrast to previous results, it appears to be more challenging to learn the correct HPI values on real HPO-MO tasks, resulting in a smaller difference between ParEGO and HPI-ParEGO. This can be especially seen on the rbv2_ranger tasks, which contain conditional configuration spaces, making the problem more complex. Nevertheless, HPI-ParEGO is the best optimizer, as soon as it surpasses MO-TPE at approximately 20% of the trials for both scenarios. We highlight that although MO-TPE is stronger on PyMOO, HPI-ParEGO is consistently and robustly performing very well on both benchmarks. Appendix E shows the difference between the HPI-ParEGO and ParEGO optimizers per YAHPO-Gym scenario.

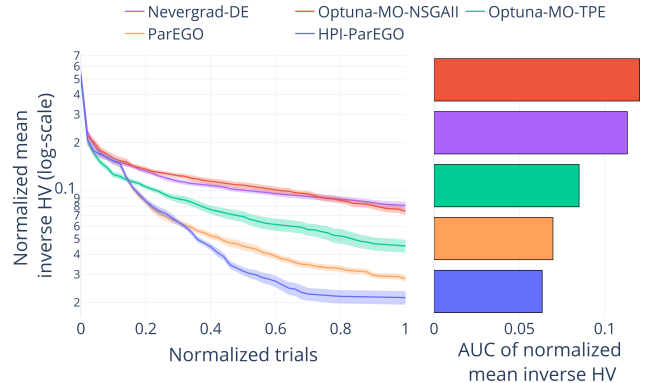


Figure 7: Results of the HPI-ParEGO optimizer compared to the baseline optimizers on the selected LCBench tasks.

5 Discussion

In this work, we proposed a novel extension to ParEGO that incorporates dynamic hyperparameter importance (HPI) estimation into the optimization loop. Our method leverages the scalarization mechanism inherent in ParEGO to identify and prioritize the most influential hyperparameters under varying trade-offs between objectives. Through extensive experiments on PyMOO and YAHPO-Gym, spanning synthetic and real-world multi-objective tasks, we demonstrated that HPI-ParEGO consistently outperforms standard ParEGO and most of our baseline optimizers, both in convergence speed and final hypervolume. Evidently, our hypothesis turned out to be

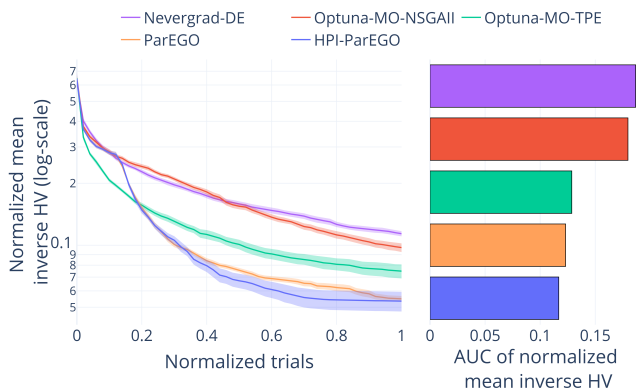


Figure 8: Results of the HPI-ParEGO optimizer compared to the baseline optimizers on the selected `rbv2_ranger` tasks.

true: Many hyperparameters contribute little to performance under specific objective trade-offs, and dynamically filtering these during optimization helps the optimizer focus its budget on the relevant subspace.

A full theoretical understanding of when importance-guided filtering benefits MOO remains open. Our preliminary understanding suggests that in applications with many unimportant hyperparameters, HPI-ParEGO is more effective at quickly identifying them. However, a strongly varying HPI with many slightly important hyperparameters is harder to learn under a restricted optimization budget.

Nevertheless, our results clearly show that HPI should not remain a post-hoc diagnostic tool, but can be actively used during optimization, as previous work has done for single-objective optimization [Wang *et al.*, 2021], even in multi-objective scenarios. This opens up a new class of resource-efficient MOO methods that can be, for example, important for Green AI and Green AutoML, emphasizing lower compute cost and reduced energy consumption without sacrificing accuracy [Tornede *et al.*, 2023].

Limitations and Future Work. Despite its empirical performance, our approach has some limitations that suggest caution and offer directions for future improvement. The effectiveness of dynamic HPI estimation relies heavily on the accuracy of the surrogate model. In early iterations, surrogate predictions may be inaccurate, potentially leading to unreliable importance scores [Wever *et al.*, 2026]. Although we mitigate this with random augmentation and delayed subsampling, this remains a bottleneck in data-scarce scenarios. Related to this, for very few trials, the τ -schedule (i.e., when to perform HPI reduction) might not work well because the reduction occurs too early when the surrogate model is not yet well-trained. In addition, the performance and surrogate model quality may degrade as the dimensionality of the configuration space grows, making it too slow in practice for very large-scale problems. In particular, our approach using HyperSHAP could create too much overhead for HPO tasks with tens or hundreds of hyperparameters, e.g., for optimizing large pipelines as in Auto-Sklearn [Feurer *et al.*, 2015].

In view of this limitation, there are several opportunities for future work to overcome these limitations: (i) exploration

of more robust and uncertainty-aware HPI estimation techniques, for example, using stochastic Shapley values [Chau *et al.*, 2023]; (ii) meta-learning of HPI priors from previous HPO tasks; or (iii) adapting τ in a data-driven way.

Furthermore, we address the black-box problem of HPO in our paper. Due to the high cost of model training (e.g., in deep learning), a common approach is to use multi-fidelity optimization [Swersky *et al.*, 2014; Falkner *et al.*, 2018; Li *et al.*, 2020; Bohdal *et al.*, 2023] to early stop unpromising runs. It is an open research problem how much information, e.g., on HPI, can be leveraged from cheap training runs to improve optimization efficiency. Results from Zimmer *et al.* [2021] suggest that HPI might be stable enough to be leveraged at least on simple DNNs.

Our method is currently tailored to scalarization-based optimizers such as ParEGO. While this choice enables seamless integration with HPI estimation, it limits generality. Extending the method to other MOO paradigms, such as nondominated-sorting-based evolutionary algorithms, requires rethinking how HPI is computed and applied. One possible approach is to use hypervolume for HyperSHAP to determine the importance of hyperparameters across the entire Pareto front, rather than just the current objective trade-off.

Our evaluation does not cover many-objective optimization scenarios with more than three objectives, which present distinct challenges and dynamics, and these settings remain an open question for future research. This goes hand in hand with the limitation of our approach to ParEGO-like algorithms, because the sequential nature and ParEGO’s surrogate model are rather meant for restricted optimization budgets. However, many-objective problems often require much larger optimization budgets to sufficiently learn what the Pareto front looks like. Thus, we have not addressed many-objective optimization in this paper. Therefore, we see extensions of our idea to NSGA-III [Deb and Jain, 2014] and the population-based contexts as promising future work.

Broader Impact. Improving the efficiency of multi-objective HPO can reduce the computation and environmental costs. By focusing the search on the most relevant hyperparameters, our method has the potential to lower resource consumption without sacrificing performance, making it particularly relevant for sustainable AI. Moreover, our work can help democratize access to HPO by making it more accessible to practitioners with limited computational budgets.

However, like all optimization techniques, this approach may inadvertently encode biases present in the data or objectives, especially when fairness or safety is one of the target objectives. Along the same lines, automation bias in the development of new ML applications could be higher risk when using AutoML method such as ours. We encourage practitioners to carefully consider the choice of objectives and the implications of weighting them during the optimization.

References

- M. Adachi, B. Planden, D. Howey, K. Muandet, M. Osborne, and S. Chau. Looping in the human: Collaborative and explainable bayesian optimization. *CoRR*, abs/2310.17273, 2023.
- T. Akiba, S. Sano, T. Yanase, T. Ohta, and M. Koyama. Optuna: A next-generation Hyperparameter Optimization framework. In *Proc. of KDD'19*, pages 2623–2631, 2019.
- S. Basu, F. Hutter, and D. Stoll. Multi-objective hyperparameter optimization in the age of deep learning. *arXiv preprint arXiv:2511.08371*, 2025.
- C. Benjamins, H. Graf, S. Segel, D. Deng, T. Ruhkopf, L. Hennig, S. Basu, N. Mallik, E. Bergman, D. Chen, F. Clément, M. Feurer, K. Eggenberger, F. Hutter, C. Dorr, and M. Lindauer. carps: A framework for comparing N hyperparameter optimizers on M benchmarks. *CoRR*, abs/2506.06143, 2025.
- J. Bergstra and Y. Bengio. Random search for hyperparameter optimization. *Journal of Machine Learning Research*, 13:281–305, 2012.
- A. Biedenkapp, M. Lindauer, K. Eggenberger, C. Fawcett, H. Hoos, and F. Hutter. Efficient parameter importance analysis via ablation with surrogates. In *Proc. of AAAI'17*, pages 773–779, 2017.
- A. Biedenkapp, J. Marben, M. Lindauer, and F. Hutter. CAVE: Configuration assessment, visualization and evaluation. In *Proc. of LION'18*, 2018.
- B. Bischl, M. Binder, M. Lang, T. Pielok, J. Richter, S. Coors, J. Thomas, T. Ullmann, M. Becker, A.-L. Boulesteix, D. Deng, and M. Lindauer. Hyperparameter optimization: Foundations, algorithms, best practices, and open challenges. *Wiley Interdisciplinary Reviews: Data Mining and Knowledge Discovery*, page e1484, 2023.
- J. Blank and K. Deb. pymoo: Multi-objective optimization in python. *IEEE Access*, 8:89497–89509, 2020.
- O. Bohdal, L. Balles, M. Wistuba, B. Ermis, C. Archambeau, and G. Zappella. PASHA: Efficient HPO and NAS with progressive resource allocation. In *Proc. of ICLR'23*, 2023.
- E. Bradford, A. Schweidtmann, and A. Lapkin. Efficient multiobjective optimization employing gaussian processes, spectral sampling and a genetic algorithm. *J. Glob. Optim.*, 71(2):407–438, 2018.
- S. L. Chau, K. Muandet, and D. Sejdinovic. Explaining the uncertain: stochastic shapley values for gaussian process models. In *Proceedings of the 37th International Conference on Neural Information Processing Systems, NIPS'23*, Red Hook, NY, USA, 2023. Curran Associates Inc.
- K. Deb and H. Jain. An evolutionary many-objective optimization algorithm using reference-point-based nondominated sorting approach, part i: Solving problems with box constraints. *IEEE Transactions on Evolutionary Computation*, 18(4):577–601, 2014.
- K. Deb, A. Pratap, S. Agarwal, and T. Meyarivan. A fast and elitist multiobjective genetic algorithm: Nsga-ii. *IEEE Transactions on Evolutionary Computation*, 6(2):182–197, 2002.
- K. Eggenberger, P. Müller, N. Mallik, M. Feurer, R. Sass, A. Klein, N. Awad, M. Lindauer, and F. Hutter. HPOBench: A collection of reproducible multi-fidelity benchmark problems for HPO. In *Proc. of NeurIPS'21 Datasets and Benchmarks Track*, 2021.
- T. Elsken, J. Metzen, and F. Hutter. Efficient multi-objective Neural Architecture Search via Lamarckian evolution. In *Proc. of ICLR'19*, 2019.
- S. Falkner, A. Klein, and F. Hutter. BOHB: Robust and efficient Hyperparameter Optimization at scale. In *Proc. of ICML'18*, pages 1437–1446, 2018.
- C. Fawcett and H. Hoos. Analysing differences between algorithm configurations through ablation. *Journal of Heuristics*, 22(4):431–458, 2016.
- M. Feurer and F. Hutter. Hyperparameter Optimization. In F. Hutter, L. Kotthoff, and J. Vanschoren, editors, *Automated Machine Learning: Methods, Systems, Challenges*, chapter 1, pages 3 – 38. Springer, 2019. Available for free at <http://automl.org/book>.
- M. Feurer, A. Klein, K. Eggenberger, J. Springenberg, M. Blum, and F. Hutter. Efficient and robust automated machine learning. In *Proc. of NeurIPS'15*, pages 2962–2970, 2015.
- D. Fudenberg and J. Tirole. *Game theory*. MIT press, 1991.
- F. Hutter, H. Hoos, and K. Leyton-Brown. Identifying key algorithm parameters and instance features using forward selection. In *Proc. of LION'13*, pages 364–381, 2013.
- F. Hutter, H. Hoos, and K. Leyton-Brown. An efficient approach for assessing hyperparameter importance. In *Proc. of ICML'14*, pages 754–762, 2014.
- D. Jones, M. Schonlau, and W. Welch. Efficient global optimization of expensive black box functions. *Journal of Global Optimization*, 13:455–492, 1998.
- J. D. Knowles. ParEGO: a hybrid algorithm with on-line landscape approximation for expensive multiobjective optimization problems. *IEEE Transactions on Evolutionary Computation*, 10(1):50–66, 2006.
- J. Lee, S. Ahn, H. Kim, and J. Ruth Lee. Dynamic hyperparameter allocation under time constraints for automated machine learning. *Intelligent Automation & Soft Computing*, 31(1):255–277, 2022.
- L. Li, K. Jamieson, A. Rostamizadeh, E. Gonina, J. Bentzur, M. Hardt, B. Recht, and A. Talwalkar. A system for massively parallel hyperparameter tuning. In *Proc. of ML-Sys'20*, 2020.
- M. Lindauer, K. Eggenberger, M. Feurer, A. Biedenkapp, D. Deng, C. Benjamins, T. Ruhkopf, R. Sass, and F. Hutter. SMAC3: A versatile bayesian optimization package for Hyperparameter Optimization. *Journal of Machine Learning Research*, 23(54):1–9, 2022.

- J. Lévesque, C. Gagné, and R. Sabourin. Bayesian Hyperparameter Optimization for Ensemble Learning. In *Proc. of UAI'16*, pages 437–446, 2016.
- A. Morales-Hernández, I. Van Nieuwenhuysse, and S. Gonzalez. A survey on multi-objective hyperparameter optimization algorithms for machine learning. *Artificial Intelligence Review*, 56:8043–8093, 2022.
- C. Moussa, Y. J. Patel, V. Dunjko, T. Bäck, and J. N. van Rijn. Hyperparameter importance and optimization of quantum neural networks across small datasets. *Machine Learning*, 113(4):1941–1966, 2024.
- Y. Ozaki, Y. Tanigaki, S. Watanabe, and M. Onishi. Multiobjective tree-structured parzen estimator for computationally expensive optimization problems. In *Proc. of GECCO'20*, page 533–541, 2020.
- V. Pareto. *Manual of Political Economy*. Augustus M. Kelley, New York, 1971. Originally published in Italian as *Manuale di Economia Politica*, 1906.
- F. Pfisterer, L. Schneider, J. Moosbauer, M. Binder, and B. Bischl. YAHPO Gym – an efficient multi-objective multi-fidelity benchmark for hyperparameter optimization. In *Proc. of AutoML Conf'22*. PMLR, 2022.
- P. Probst, A. Boulesteix, and B. Bischl. Tunability: Importance of hyperparameters of machine learning algorithms. *Journal of Machine Learning Research*, 20(53):1–32, 2019.
- J. Rapin and O. Teytaud. Nevergrad-a gradient-free optimization platform, 2018.
- J. Rodemann, F. Croppi, P. Arens, Y. Sale, J. Herbringer, B. Bischl, E. Hüllermeier, T. Augustin, C. Walsh, and G. Casalicchio. Explaining bayesian optimization by shapley values facilitates human-ai collaboration. *CoRR*, abs/2403.04629, 2024.
- R. Schmucker, M. Donini, V. Perrone, M. Zafar, and C. Archambeau. Multi-objective multi-fidelity hyperparameter optimization with application to fairness. In *MetaLearn'20*, 2020.
- L. S. Shapley. 17. *A Value for n-Person Games*, pages 307–318. Princeton University Press, Princeton, 1953.
- J. Snoek, H. Larochelle, and R. Adams. Practical Bayesian optimization of machine learning algorithms. In *Proc. of NeurIPS'12*, pages 2960–2968, 2012.
- N. Srinivas, A. Krause, S. Kakade, and M. Seeger. Gaussian process optimization in the bandit setting: No regret and experimental design. In *Proc. of ICML'10*, pages 1015–1022, 2010.
- K. Swersky, J. Snoek, and R. Adams. Freeze-thaw Bayesian optimization. *arXiv:1406.3896 [stats.ML]*, 2014.
- D. Theodorakopoulos, F. Stahl, and M. Lindauer. Hyperparameter importance analysis for multi-objective automl. In *Proc. of ECAI'24*, pages 1100–1107, 2024.
- T. Tornede, A. Tornede, J. Hanselle, F. Mohr, M. Wever, and E. Hüllermeier. Towards green automated machine learning: Status quo and future directions. *Journal of Artificial Intelligence Research*, 77:427–457, 2023.
- J. van Rijn and F. Hutter. Hyperparameter importance across datasets. In *Proc. of KDD'18*, pages 2367–2376, 2018.
- C. Wang, H. Wang, C. Zhou, and H. Chen. Experience-thinking: Constrained hyperparameter optimization based on knowledge and pruning. *Knowledge-Based Systems*, 223:106602, 2021.
- R. Wang, I. Nabney, and M. Golbabaee. Grouped sequential optimization strategy - the application of hyperparameter importance assessment in deep learning. In *Proceedings of Conference on Parsimony and Learning 2025*, Proceedings of Machine Learning Research, 2025. Conference on Parsimony and Learning (CPAL) ; Conference date: 24-03-2025 Through 28-03-2025.
- H. Weerts, F. Pfisterer, M. Feurer, K. Eggenberger, E. Bergman, N. Awad, J. Vanschoren, M. Pechenizkiy, B. Bischl, and F. Hutter. Can fairness be automated? guidelines and opportunities for fairness-aware automl. *Journal of Artificial Intelligence Research*, 79:639–677, 2024.
- M. Wever, M. Muschalik, F. Fumagalli, and M. Lindauer. Hypershap: Shapley values and interactions for hyperparameter importance. In *Proc. of AAAI'26*, 2026.
- M. Wistuba, N. Schilling, and L. Schmidt-Thieme. Hyperparameter search space pruning - A new component for sequential model-based hyperparameter optimization. In *Proc. of ECML/PKDD'15*, pages 104–119, 2015.
- Y. Zhao Yiyang, L. Wang, K. Yang, T. Zhang, T. Guo, and Y. Tian. Multi-objective optimization by learning space partition. In *International Conference on Learning Representations*, 2021.
- Q. Zhang and H. Li. MOEA/D: A multiobjective evolutionary algorithm based on decomposition. *IEEE Trans. Evol. Comput.*, 11(6):712–731, 2007.
- L. Zimmer, M. Lindauer, and F. Hutter. Auto-Pytorch: Multi-fidelity metalearning for efficient and robust AutoDL. *IEEE Transactions on Pattern Analysis and Machine Intelligence*, 43:3079–3090, 2021.
- E. Zitzler, K. Deb, and L. Thiele. Comparison of multiobjective evolutionary algorithms: Empirical results. *Evolutionary computation*, 8(2):173–195, 2000.

A Selection of YAHPO-Gym Tasks

We selected the tasks for LCBench and `rbv2_ranger` by randomly drawing 20 different weight vectors and applying HyperSHAP to the surrogate models provided by YAHPO-Gym [Pfisterer *et al.*, 2022], combining multiple objectives as originally defined by Knowles [2006]. While for `rbv2_ranger`, we consider accuracy and memory as objectives, LCBench tasks have been run considering validation accuracy and time. To this end, we considered the tunability of these weightings with respect to the default configuration as a baseline. Based on these results, we apply our hyperparameter selection method to determine a subset of hyperparameters worth tuning for a specific weight vector. Afterward, we selected the top 13 tasks for LCBench and `rbv2_ranger` that maximize the number of different subsets of hyperparameters for different weight vectors. Additionally, we paid attention that the subsets of hyperparameters actually differ across different weightings.

B Hardware Setup

The computations were conducted on a high-performance computer with nodes equipped with $2 \times$ AMD Milan 7763 (2×64 cores) and 256GiB RAM each, running Red Hat Enterprise Linux Ootpa and Slurm. Of that, 1 cores and 16GB RAM have been allocated to the execution of a single run.

C Number of Trials per Task

In YAHPO-Gym paper Pfisterer *et al.* [2022], the number of trials is defined as $\text{number of trials} = 20 + 40\sqrt{D}$ with D being the number of dimensions. For our LCBench, `rbv2_ranger`, and PyMOO, we used five times as many trials. We ran the PyMOO tasks ZDT1–3 only for three times as many trials, since they are computationally expensive.

D Ablation Study Variants

In an ablation study, we tried variants of our algorithm. All options are shown in Table 1 in Section 4.3 and will be described here in more detail. All comparisons were performed with the setup of the HPI-ParEGO optimizer (configspace adjustment value: incumbent, threshold: Symmetric-0.8, $r=0.1$, $u=10$). For the ablation experiments, we used three tasks from each LCBench and `rbv2_ranger`, which were not part of the final evaluation.

D.1 HPI Implementation Details

To integrate HyperSHAP, we use the HyperSHAP library [Wever *et al.*, 2026] version 0.0.6, which is available as a PyPI package and on GitHub (<https://github.com/automl/hypershap>). It generates some random configurations as input to the current surrogate model and uses these to estimate the Shapley values. We use the tunability estimation with the index set to Shapely values and an order of 1, as calculating higher-order interactions would be too resource-intensive for this method, given that the importance is recalculated many times.

D.2 Threshold Ablation

Next to the current threshold, we ablated over two additional options, where we make changes after every 33% of the optimization trials. The motivation for the initialization phase is that we start with (almost) all hyperparameters to first learn which ones are important and improve the surrogate model, and then focus more and more on the important ones. The motivation behind the convergence phase is to allow the optimizer to tune the less important hyperparameters in the end as well. For the symmetric threshold, we combine the intuition by letting the optimizer explore the space initially, then narrowing it down, and finally allowing for more exploration at the end again to make sure the entire space could be covered. Figure 9 shows the results of the threshold comparison, which shows that the symmetric schedule is the best, closely followed by a constant threshold.

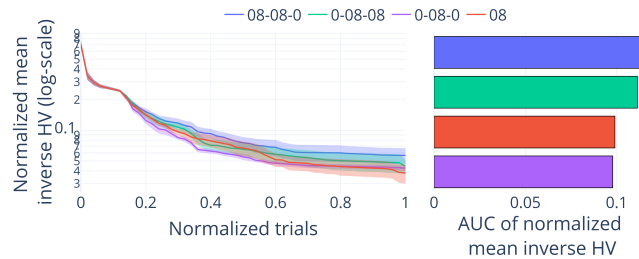


Figure 9: Ablation results for different thresholds. 0 means no reduction.

D.3 Random Probability for HPI

We also considered different values for the random chance r that a random configuration of the original configuration space will be evaluated. We tested: 0.0, 0.1, 0.2. The results are shown in Figure 10. It can be seen that sometimes using random, full configurations has a small but positive effect.

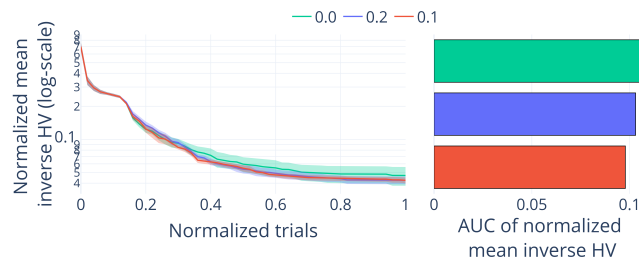


Figure 10: Ablation results for different random chances r .

D.4 Number of Iterations u for a Weight Update

The intuition behind increasing the number of iterations for a weight update in comparison to the original ParEGO algorithm is that the optimization process can focus on a scalarization for more iterations and thereby improve on the current scalarization. This also allows for leveraging the reduced configuration space several times before it is reset. We tested different values: 6, 10, and 20. Figure 11 shows that every 10 iterations is a good value.

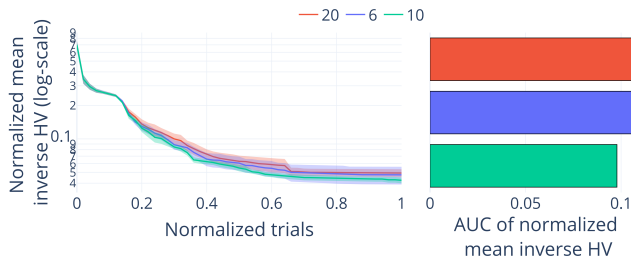


Figure 11: Ablation results for different numbers of iterations for weight updates u .

E Task Difference for the Selected YAHPO-Gym Tasks

Figure 12 and Figure 13 compare HPI-ParEGO and the ParEGO baseline across the different scenarios from YAHPO-Gym. The results reveal that the benefits of incorporating hyperparameter importance are not uniform: while HPI-ParEGO achieves clear improvements on LCBench, its advantage is less consistent on `rbv2_ranger`, where for some tasks it clearly performs better, for others ParEGO is better. This variation highlights that the effectiveness of HPI-guided optimization can depend on task characteristics, such as the dimensionality of the configuration space and the presence of conditions within it. As shown in Figure 7 and 8 in Section 4.4, HPI-ParEGO performs overall better than the standard ParEGO.

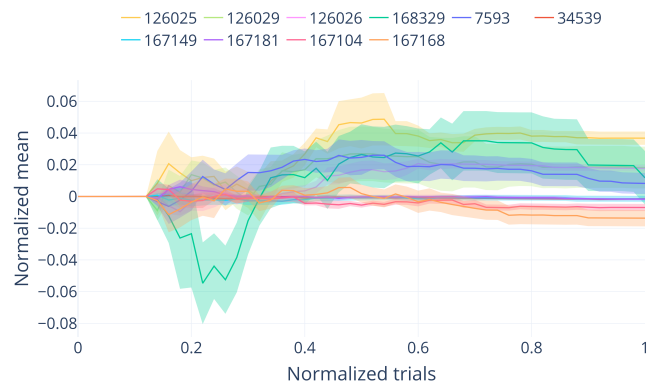


Figure 12: Results of the difference per task of the HPI-ParEGO optimizer compared to the baseline optimizer on the selected LCBench tasks. A positive value means an advantage of HPI-ParEGO over the baseline, and vice versa.

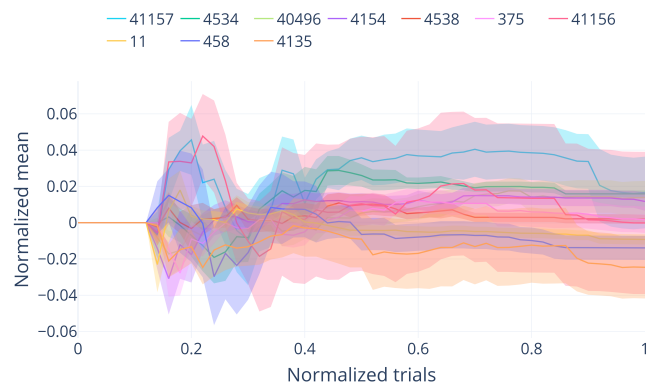


Figure 13: Results of the difference per task of the HPI-ParEGO optimizer compared to the baseline optimizer on the selected `rbv2_ranger` tasks